Journal of Chromatography A, 1218 (2011) 6419–6425

Contents lists available at ScienceDirect

Journal of Chromatography A

journal homepage: www.elsevier.com/locate/chroma

Zwitterionic-type hydrophilic interaction nano-liquid chromatography of complex and high mannose glycans coupled with electrospray ionisation high resolution time of flight mass spectrometry

Lea Mauko[a], Matthias Pelzing[b], Sebastiaan Dolman[b], Anna Nordborg[a], Nathan A. Lacher[c], Paul R. Haddad[a], Emily F. Hilder[a,*]

[a] Pfizer Analytical Research Centre (PARC), Australian Centre for Research on Separation Science (ACROSS), School of Chemistry, University of Tasmania, Private Bag 75, Hobart, Tasmania 7001, Australia
[b] Bruker Biosciences, Preston, Victoria, Australia
[c] Analytical R&D, Pfizer BioTherapeutics Pharmaceutical Sciences, Chesterfield, MO, USA

ARTICLE INFO

Article history:
Received 31 May 2011
Received in revised form 1 July 2011
Accepted 4 July 2011
Available online 12 July 2011

Keywords:
Monoclonal antibodies
Glycans
Nano liquid chromatography
ZIC-HILIC
Nano ESI-MS

ABSTRACT

In this study we describe a new method for rapid and sensitive analysis of reduced high mannose and complex glycans using zwitterionic-type hydrophilic interaction nano-liquid chromatography (nano ZIC-HILIC, 75 μm I.D. × 150 mm) coupled with high resolution nanoelectrospray ionisation time of flight mass spectrometry (nano ESI-TOF-MS). The retention of neutral glycans increases with increasing molecular weight and is higher for high mannose glycans than for complex-type glycans. The selectivity of ZIC-HILIC for sialylated glycans differs from that for the neutral glycans and is believed to involve electrostatic repulsion; therefore, charged glycans are eluted earlier than neutral glycans with comparable molecular weight. Due to the improved sensitivity achieved by employing a ZIC-HILIC nano-column, a range of less common complex glycans has been studied and the high resolution mass spectrometry enabled confirmation of glycan composition for the proposed structures. Good sensitivity for glycans was achieved without prior fluorescent labelling, and the time of the analysis was significantly reduced compared to the separation of glycans on a conventional-size column. The proposed method offers a fast and sensitive approach for glycan profiling applied to analysis of biopharmaceuticals.

1. Introduction

Glycosylation is a very versatile posttranslational modification; it contributes to the complexity of protein molecules and it determines the biological activity and the function of proteins [1,2]. A strong correlation has been found between changes in glycosylation patterns and some pathological states [3]. Identification of proteins, glycosylation sites, and glycan heterogeneity are the main challenges of the glycoproteomic field [4]. Understanding the biological processes also provides new strategies for designing more specific and more potent biopharmaceuticals which are already one of the fastest growing therapeutic areas. The main emphasis in this arena is in development of recombinant monoclonal antibodies (MAbs) expressed in various mammalian systems which can produce alternative glycosylation patterns to that of humans [5]. It has been shown that the glycosylation determines activity, stability, and immunogenicity of the MAbs and the new generation of drugs will most likely exhibit a more uniform glycosylation pattern with controlled production of sialylated and fucosylated species [6,7].

The most common strategy in the analysis of N-glycans involves digestion with the enzyme PNGase F and labelling of released glycans with a fluorescent tag via reductive amination followed by the reversed phase or hydrophilic interaction liquid chromatography (HILIC) coupled with fluorescence detection [8,9]. The main advantage of this approach is high sensitivity and the possibility of relative quantification. The most commonly used fluorescent labels are 2-aminobenzamide (2-AB), 2-aminopyridine and 2-anthranilic acid (2-AA) [10–14]. The 2-AB label is used widely for separations in the HILIC mode and databases for structural assignment of glycans are readily available [11,15]. Due to the charged functional group, 2-AA labelled glycans can also be separated with capillary electrophoresis [16]. However, the fluorescent labelling is expensive and time consuming and fluorescence detection does not provide direct structural information. For the separation of native and reduced N-glycans, graphitized carbon columns coupled with MS detection are commonly used [17–19]. Recently, the

* Corresponding author at: Australian Centre for Research on Separation Science (ACROSS), School of Chemistry, University of Tasmania, Sandy Bay, Private Bag 75, Hobart 7001, Australia. Tel.: +61 03 62267670; fax: +61 03 62262858.
E-mail address: Emily.Hilder@utas.edu.au (E.F. Hilder).

0021-9673/$ – see front matter © 2011 Elsevier B.V. All rights reserved.
doi:10.1016/j.chroma.2011.07.006

use of zwitterionic-type hydrophilic interaction liquid chromatography (ZIC-HILIC) for the separation of reduced glycans released from MAbs has been reported [20]. ZIC-HILIC stationary phases have also been applied to analysis of fluorescently labelled glycans [10] and glycopeptides, either for solid-phase extraction and sample enrichment [21,22], or separation of glycopeptides [22,23]. Due to enhanced capability for recognition of glycans and glycopeptides, it is believed that ZIC-HILIC may gain more popularity in the future.

Another widely used method for glycosylation analysis is capillary electrophoresis (CE), either coupled with laser-induced fluorescence (LIF) or mass spectrometry (MS) detection [24] or using a combination of CE-LIF-MS [25]. Analysis of glycans by CE requires derivatisation of glycans with multiply charged fluorescent labels to provide suitable electrophoretic mobility and improve sensitivity. However, charged glycans, such as sialic acids, can be successfully analysed by CE-MS without prior labelling [26]. In combination with high resolution MS, CE has also been applied to the determination of modifications of intact recombinant glycoproteins [27].

An alternative strategy for glycan profiling with improved sensitivity is the separation of underivatised glycans using nanoscale liquid chromatography (LC) coupled with mass spectrometric detection. Nanoscale graphitized carbon and HILIC amide stationary phases have been used for the separation of underivatised O- and N-glycans with low-femtomole sensitivity [28–32]. The nanoscale graphitized carbon columns have also been used in a microchip format [33]. Recently, a chip-based reversed phase LC separation of permethylated glycans has also been reported [34]. The use of porous layer open tubular HILIC columns with 10 μm I.D. for sensitive glycan analysis with ESI-MS detection has also been demonstrated [35].

In this paper we demonstrate the use of a ZIC-HILIC nanocolumn for a simple, rapid, and sensitive analysis of reduced high mannose and complex glycans from ribonuclease B and a recombinant monoclonal antibody. With this new method, higher sensitivity was achieved compared to the conventional approach previously reported by our group [20]. The ZIC-HILIC column exhibited different selectivity for neutral and sialylated glycans and a wide range of charged minor glycan species was identified. The nano ZIC-HILIC was coupled to a high resolution mass spectrometer which enabled study of structures that could not previously be identified by any current conventional approach.

2. Materials and methods

2.1. Reagents and chemicals

Unless otherwise noted all chemicals were of analytical reagent grade. Acetonitrile, ammonium hydroxide, ammonium bicarbonate and acetic acid were purchased from Fluka (Buchs, Switzerland). Ethanol, ribonuclease B (RNase B, R7884) and sodium borohydride were obtained from Sigma (St. Louis, MO, USA). Monoclonal antibody prepared by recombinant DNA technology was donated by Pfizer Inc. (St. Louis, MO, USA).

2.2. Sample preparation

Glycoprotein samples (250 μg) were desalted prior to digestion using centrifugal filter units (Amicon Ultra, 10.000 MWCO, Millipore, Carrigtwohill, Ireland). Glycans were released from glycoproteins by digestion with 3 μL of PNGase F (500 units/mL, from Elizabethkingia meningoseptica; Sigma) per 100 μL of glycoprotein solution in 50 mM ammonium bicarbonate buffer, pH 8.0, overnight at 37 °C. Proteins were removed by precipitation with 400 μL of ice-cold ethanol and dried in the vacuum oven overnight at 40 °C. The dried supernatants were reduced by adding 20 μL of 0.5 M sodium borohydride in 50 mM sodium hydroxide and incubating at room temperature overnight. The samples were then acidified by adding 5 μL of glacial acetic acid and desalted by ion-exchange chromatography (Dowex MR-3 mixed bed, Sigma). Prior to analysis, the samples were diluted by a factor of ten in acetonitrile and 2 μL of the sample was injected onto the column.

2.3. Nano ZIC-HILIC coupled with nano ESI-MS

Nano ZIC-HILIC chromatography was performed with a Merck SeQuant (Umeå, Sweden) nano ZIC-HILIC column (75 μm I.D. × 150 mm) with 5 μm particle size. The analyses were performed on a Dionex Ultimate 3000 HPLC system, including a ternary low-pressure-mixing gradient pump (DGP-3600) equipped with a membrane degasser unit (SRD-3600), a temperature-controlled column oven with a flow manager (FLM-3100) and a thermostated autosampler (WPS-3000T). Mobile phase A and B consisted of acetonitrile and 2 mM ammonium acetate in water, pH 6.9, respectively. The flow-rate was set to 600 nL/min and the temperature of the column was maintained at 40 °C. Ribonuclease B and MAb glycans were analysed using gradient elution, starting with a 3 min isocratic step at 10% B, followed by a linear gradient from 10 to 45% B in 15 min and finished with a wash step at 95% B for 5 min. Prior to the next injection, the column was equilibrated for 25 min at 10% B. The LC system was coupled to the high resolution orthogonal TOF-MS (MaXis, Bruker-Daltonik, Bremen, Germany). The transfer capillary was kept at a voltage of −4500 V (positive ion polarity mode) or 3500 V (negative ion polarity), respectively. The nebulizer was set to 0.6 bar using ESI nano-sprayer (Bruker, Bremen, Germany), the dry gas temperature to 180 °C and the dry gas flow-rate to 3 L/min. The ion transfer was optimized in the range m/z 200–3000 for highest sensitivity while keeping the resolution R > 50,000 across the whole mass range. The TOF-MS mass calibration was carried out prior the LC–MS experiment by direct infusion of a 100 fold dilution of ES Tuning Mix (Agilent Technologies, Waldbronn, Germany) at 4 μL/min.

3. Results and discussion

3.1. Separation of high mannose glycans released from RNase B

RNase B is a glycoprotein with a molecular weight of approximately 15 kDa containing a single N-linked glycosylation site for high mannose glycans with 5–9 mannose units and several possible structural isoforms [36]. Prior to the separation, the PNGase F released glycans were reduced to avoid a complex chromatogram resulting from the presence of anomers. The glycan profile of RNase B obtained by ZIC-HILIC nano LC–ESI-TOF-MS in positive mode is shown in Fig. 1. The expected order of elution according to the glycan size was achieved; the glycans with higher molecular weight exhibited longer retention times, as summarised in Table 1. The observed behaviour was in agreement with the accepted HILIC separation mechanism. All high mannose glycans were eluted over a 3 min range and most of them were baseline resolved. Some unreduced glycans present in the sample led to additional peaks being observed in the base peak chromatogram (BPC). The high resolution of the mass spectrometer enabled a clear distinction to be made between the reduced and unreduced peaks, which can otherwise give a partially overlapping pattern. All the high mannose glycans exhibited a similar ionisation pattern, with dominating doubly charged $[M+H+NH_4]^{2+}$ ions. Singly charged protonated and sodiated molecular ion was observed for the Man5 glycan, however with increasing molecular weight the proportion of doubly charged species increased. In-source fragmentation

Table 1
Reduced glycans released from the RNase B.

Glycan composition	Structure	Abbr.	Retention time/min	Ions		$M_{theoretical}$ $[M+H]^+$/Da	$M_{measured\ deconvoluted}$ $[M+H]^+$/Da	Δmass/ppm
$(Man)_3(GlcNAc)_2$		Man3	NA	$[M+2H]^{2+}$	$[M+H]^+$	913.35071	913.35214	−1.6
$(Man)_1+(Man)_3(GlcNAc)_2$		Man4	NA	$[M+H+NH_4]^{2+}$	$[M+2H]^{2+}$ $[M+H]^+$	1075.40353	1075.40498	−1.3
$(Man)_2+(Man)_3(GlcNAc)_2$		Man5	23.8	$[M+H+NH_4]^{2+}$	$[M+2H]^{2+}$ $[M+H]^+$ $[M+Na]^+$	1237.45635	1237.45556	0.6
$(Man)_3+(Man)_3(GlcNAc)_2$		Man6	24.6	$[M+H+NH_4]^{2+}$	$[M+2H]^{2+}$ $[M+NH_4]^+$ $[M+H]^+$	1399.50918	1399.50828	0.6
$(Man)_4+(Man)_3(GlcNAc)_2$		Man7	25.2	$[M+H+NH_4]^{2+}$	$[M+2H]^{2+}$	1561.56200	1561.56185	0.1
$(Man)_5+(Man)_3(GlcNAc)_2$		Man8	25.7	$[M+H+NH_4]^{2+}$	$[M+2H]^{2+}$	1723.61482	1723.61387	0.6
$(Man)_6+(Man)_3(GlcNAc)_2$		Man9	25.9	$[M+H+NH_4]^{2+}$	$[M+2H]^{2+}$	1885.66765	1885.66682	0.4

■: N-acetylglucosamine (GlcNAc); ●: mannose (Man); NA: not assigned, only in-source fragments of larger glycans observed.

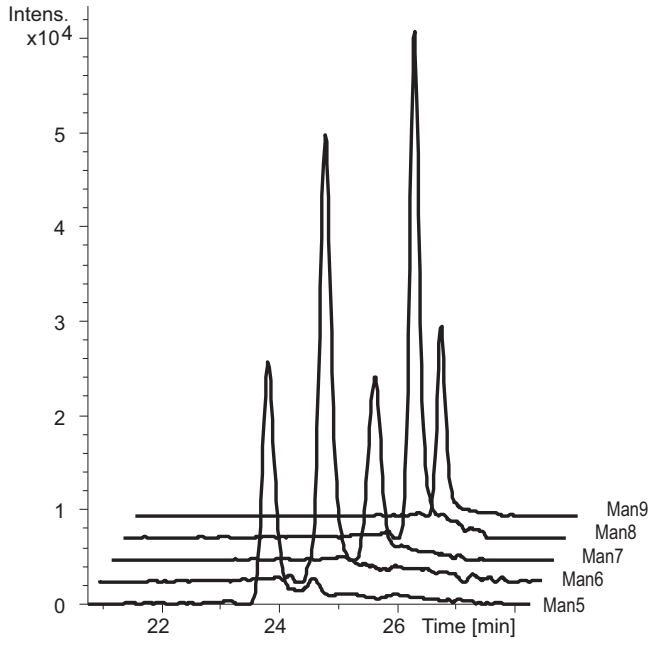

Fig. 1. Separation of reduced high mannose glycans from RNase B. Gradient elution, 10–45% B; mobile phase A (acetonitrile) and mobile phase B (2 mM ammonium acetate, pH 6.9, in water); ESI-MS, positive mode. High resolution extracted ion chromatograms (hrEIC), *m/z*: (Man5) 627.7451 ± 0.002; (Man6) 708.7715 ± 0.002; (Man7) 789.7979 ± 0.002; (Man8) 870.8243 ± 0.002; (Man9) 951.8507 ± 0.002.

was observed for singly and doubly protonated ions, with the loss of one or two mannose residues (Fig. 2). Less fragmentation was observed for $[M+H+NH_4]^{2+}$ ions which indicated the stabilizing effect of NH_4^+ ion. It has been previously reported that oligomannosidic glycans are prone to in-source fragmentation depending on the solvent composition [17]. Compared to the original procedure, the complete analysis time was reduced from 105 min for the conventional-scale method [20] to 48 min for nano ZIC-HILIC, mainly due to the steeper gradient profile, with a 70 fold increase in sensitivity which results from the lower chromatographic dilution

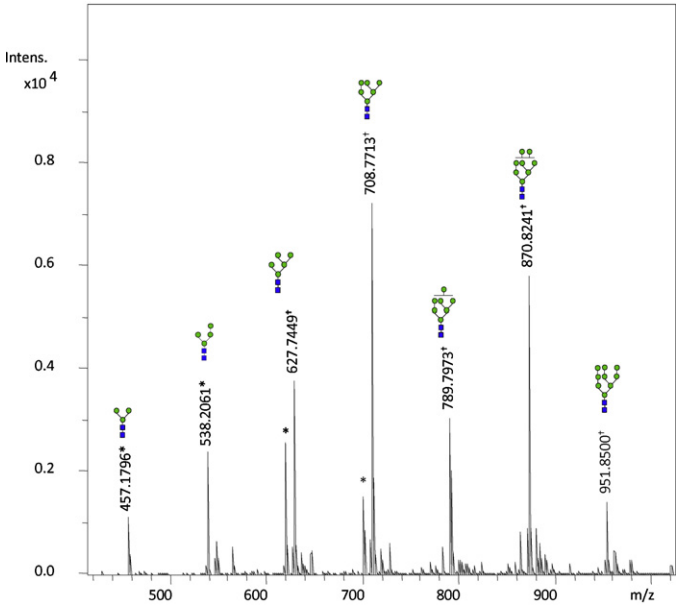

Fig. 2. Accumulated mass spectrum over the RNase B glycan elution range obtained by nano ZIC-HILIC; positive mode, background subtracted. *Doubly charged protonated species from fragment ions, †doubly charged $[M+H+HN_4]^{2+}$ species.

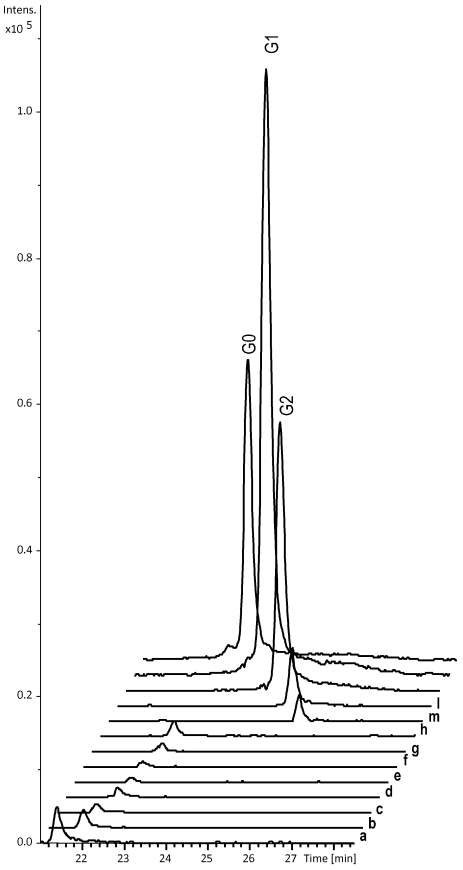

Fig. 3. Separation of reduced glycans from the MAb. Gradient elution, 10–45% B; mobile phase A (acetonitrile) and mobile phase B (2 mM ammonium acetate, pH 6.9, in water); ESI-MS, positive mode. HrEIC's of the following glycans: (a) 866.3192 ± 0.002; (b) 967.8589 ± 0.002; (c) 947.3456 ± 0.002; (d) 1048.8853 ± 0.002; (e) 955.3431 ± 0.003; (f) 1028.3720 ± 0.005; (g) 1129.9117 ± 0.005; (h) 631.7476 ± 0.002; (l) 1057.3930 ± 0.003; (m) 976.3666 ± 0.002; (G2) 895.3401 ± 0.002; (G1) 814.3137 ± 0.002; (G0) 733.2873 ± 0.002. The proposed structures are listed in Table 2.

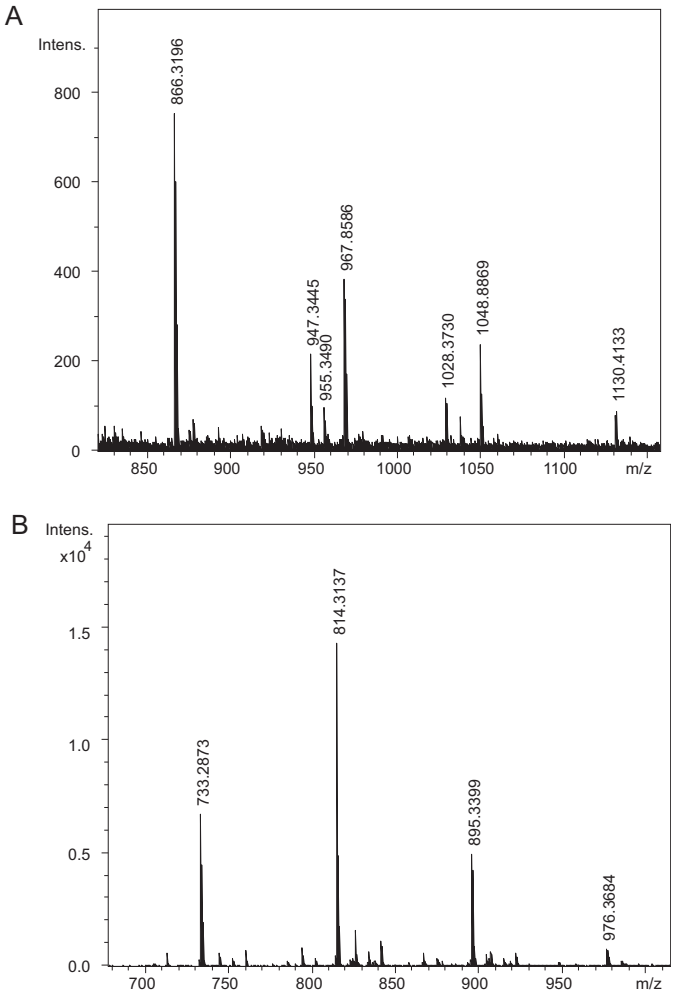

Fig. 4. Accumulated mass spectrum over the MAbsialylated (A) and neutral (B) glycan elution range obtained by nano ZIC-HILIC; positive mode, background subtracted. Doubly protonated ions $[M+2H]^{2+}$ are observed for the complex-type glycans.

of the sample. The mass sensitivity in chromatographic detection increases with the inverse square of the column diameter and lower flow-rates additionally improve the ionisation efficiency in nano ESI [37].

3.2. Separation of glycans originating from monoclonal antibody

Reduced MAb glycans were analysed using nano ZIC-HILIC coupled with ESI-TOF-MS. The same gradient conditions as for high mannose glycans were used due to expected similar retention properties, as described previously. The lower retention of complex glycans compared to the high mannose glycans with comparable mass, Fig. 3, was consistent with the results obtained on conventional size ZIC-HILIC. Using nano ZIC-HILIC, higher sensitivity compared to conventional ZIC-HILIC chromatography was achieved. The MAb glycan sample was measured in positive and negative ionisation mode which allowed identification of all previously observed glycans commonly present in this monoclonal antibody (Table 2; h–k), which are generally of the biantennary complex type. Furthermore, nine new peaks for low-abundant glycans were observed with the proposed structures summarised in Table 2 (a–g, l–m). When 2-AB labelled glycans from the same MAb were analysed by amide HILIC coupled with fluorescence detection, several minor species were observed. However, due to the lower sensitivity of MS in comparison to fluorescence detection and lack of appropriate standards, they have not been previously characterised [20].

For all the known complex glycans, the dominant ion species in the positive mode were doubly charged protonated ions (Fig. 4) which is different to the high mannose glycans, where under the same experimental conditions predominantly the $[M+H+NH_4]^{2+}$ has been observed. The difference in the ionisation pattern suggests that the formation of the pseudo molecular ions depends strongly on the structure of the glycan and it is expected that the same structural type of glycans will exhibit the same ionisation pattern. The doubly charged protonated ions could be predicted for peaks that were not previously observed using a conventional size column. Considering high mass accuracy, two possible glycans structures with the same elemental composition can be predicted for most of the observed peaks. The average error in mass determination for most of the glycans was below 2 ppm. With the achieved high mass accuracy it is possible to predict a limited number of possible structures for the observed ions. Two probable series of seven related complex and hybrid glycans which were eluted before the neutral G0, G1 and G2 glycans could be identified, either containing N-acetylneuraminic acid (NeuAc) or N-glycolylneuraminic acid (NeuGc). The combination of $Deoxyhexose_1NeuGc_1$ residues is more likely to be expected in the sample than $Hexose_1NeuAc_1$ as will be further discussed (Table 2). For the ion (e), only one possible structure can be assigned which confirms the presence of NeuGc in

Table 2
Reduced glycans released from the MAb.

Glycan composition	Structure	Abbr.	Retention time/min	Ions	$M_{theoretical}$ $[M+H]^+$/Da	$M_{measured\ deconvoluted}$ $[M+H]^+$/Da	Δmass/ppm
$(Hex)_1(HexNAc)_1(Deoxyhexose)_1(NeuGc)_1+(Man)_3(GlcNAc)_2$		a	21.4	$[M+2H]^{2+}$	1731.63114	1731.63040	0.4
$(Hex)_1(HexNAc)_2(Deoxyhexose)_1(NeuGc)_1+(Man)_3(GlcNAc)_2$	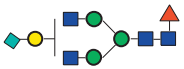	b	21.8	$[M+2H]^{2+}$	1934.71052	1934.71046	0.0
$(Hex)_2(HexNAc)_1(Deoxyhexose)_1(NeuGc)_1+(Man)_3(GlcNAc)_2$	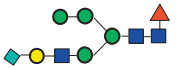	c	21.9	$[M+2H]^{2+}$	1893.68397	1893.68235	0.9
$(Hex)_2(HexNAc)_2(Deoxyhexose)_1(NeuGc)_1+(Man)_3(GlcNAc)_2$	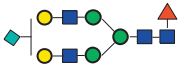	d	22.2	$[M+2H]^{2+}[M+3H]^{3+}$	2096.76334	2096.76136	0.9
$(Hex)_3(HexNAc)_1(NeuGc)_1+(Man)_3(GlcNAc)_2$	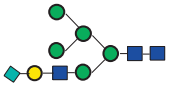	e	22.3	$[M+2H]^{2+}$	1909.67888	1909.67934	−0.2
$(Hex)_3(HexNAc)_1(Deoxyhexose)_1(NeuGc)_1+(Man)_3(GlcNAc)_2$	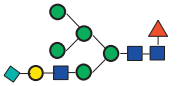	f	22.3	$[M+2H]^{2+}$	2055.73679	2055.73537	0.7
$(Hex)_3(HexNAc)_2(Deoxyhexose)_1(NeuGc)_1+(Man)_3(GlcNAc)_2$	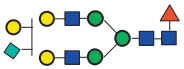	g	22.6	$[M+2H]^{2+}[M+3H]^{3+}$	2258.81616	2258.82237	−2.7
$(HexNAc)_1(Deoxyhexose)_1+(Man)_3(GlcNAc)_2$	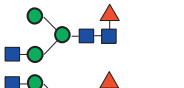	h	22.8	$[M+2H]^{2+}$	1262.48799	1262.48923	−1.0
$(HexNAc)_2(Deoxyhexose)_1+(Man)_3(GlcNAc)_2$	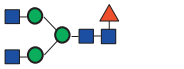	i/G0	23.5	$[M+2H]^{2+}$	1465.56736	1465.56786	−0.3
$(Hex)_1(HexNAc)_2(Deoxyhexose)_1+(Man)_3(GlcNAc)_2$	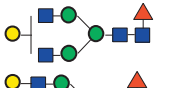	j/G1	24.1	$[M+2H]^{2+}$	1627.62018	1627.61994	0.1
$(Hex)_2(HexNAc)_2(Deoxyhexose)_1+(Man)_3(GlcNAc)_2$	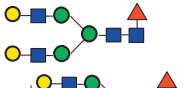	k/G2	24.7	$[M+2H]^{2+}[M+3H]^{3+}$	1789.67301	1789.67291	0.1
$(Hex)_3(HexNAc)_2(Deoxyhexose)_1+(Man)_3(GlcNAc)_2$	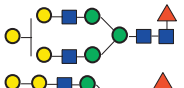	l	25.1	$[M+2H]^{2+}[M+3H]^{3+}$	1951.72583	1951.72641	−0.3
$(Hex)_4(HexNAc)_2(Deoxyhexose)_1+(Man)_3(GlcNAc)_2$	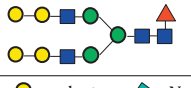	m	25.5	$[M+2H]^{2+}$ $[M+3H]^{3}$	2113.77865	2113.77827	0.2

■ : N-acetylglucosamine (GlcNAc); ● : mannose (Man); ▲ : fucose; ○ : galactose; ◆ : N-glycolylneuraminic acid (NeuGc); hexose (Hex); N-acetylhexosamine (HexNAc).

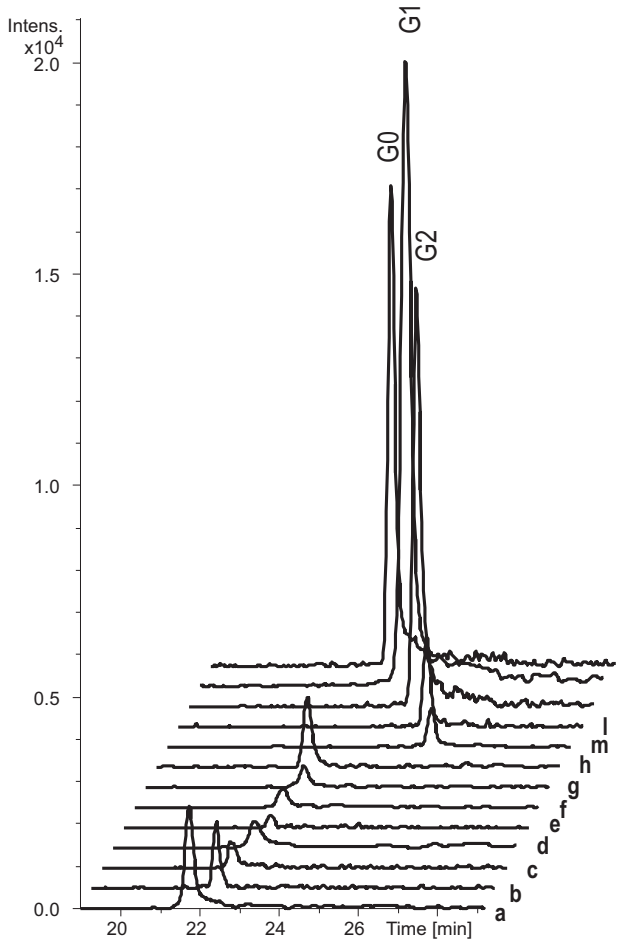

Fig. 5. Separation of reduced glycans from the MAb. Gradient elution, 10–45% B; mobile phase A (acetonitrile) and mobile phase B (2 mM ammonium acetate, pH 6.9, in water); ESI-MS, negative mode. HrEIC's from top to bottom, *m*/*z*: (a) 864.3036 ± 0.005; (b) 965.8432 ± 0.005; (c) 945.3300 ± 0.005; (d) 1046.8697 ± 0.01; (e) 953.3274 ± 0.005; (f) 1026.3564 ± 0.010; (g) 1127.8961 ± 0.01; (h) 629.7320 ± 0.005; (m) 1055.3773 ± 0.010; (l) 974.3509 ± 0.005; (G2) 893.3245 ± 0.005; (G1) 812.2981 ± 0.005; (G0) 731.2717 ± 0.005.

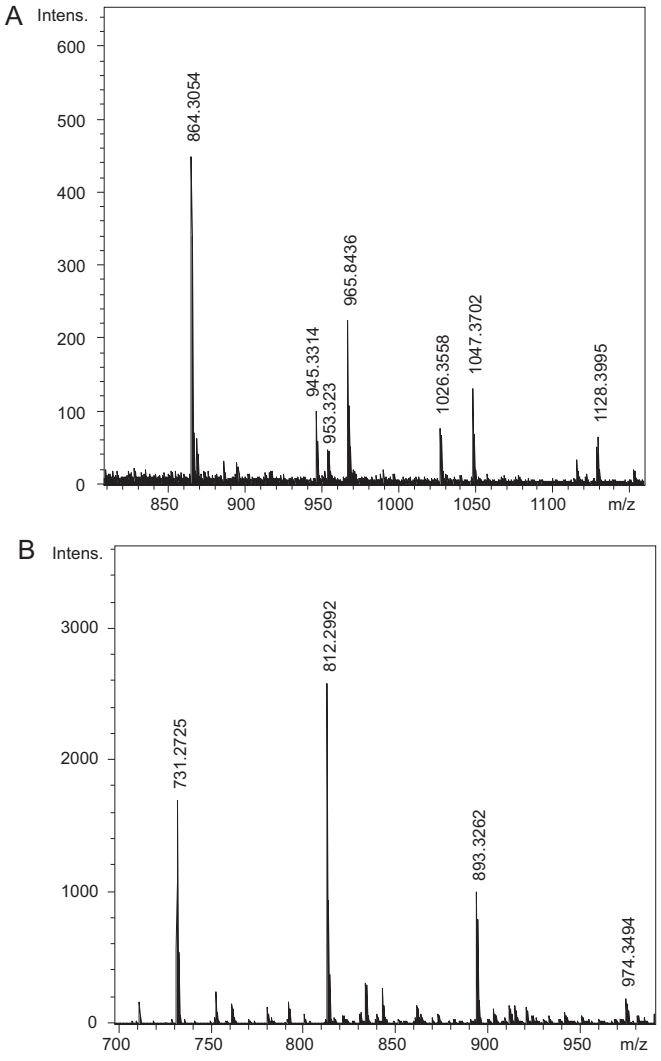

Fig. 6. Accumulated mass spectrum over the MAb sialylated (A) and neutral (B) glycan elution range obtained by nano ZIC-HILIC; negative mode, background subtracted.

the sample. This result is consistent with the fact that the MAb was expressed in a NS0 murine cell line which is known to produce glycans with a high content of NeuGc [38]. In addition, the high degree of fucosylation in the cell line producing the MAb leads us to the deduction that the glycans observed belong to the group of core-fucosylated complex and hybrid glycans containing NeuGc rather than NeuAc. The structures (a–g) in the table most likely correspond to the peaks observed in the chromatogram (Fig. 3). The relative intensities for the proposed complex sialylated glycans are higher to those of hybrid sialylated glycans (Fig. 4), which is in agreement with the high content of neutral complex glycan species in the sample. The minor glycans are being currently further analysed in combination with various exoglycosidases treatment to confirm identity of the species observed in this study and for their detailed structural elucidation.

Elution of glycans containing sialic acid prior to elution of the neutral glycans, Fig. 3 with the corresponding data summarised in Table 2, indicated that the separation of glycans was not governed by hydrophilic interaction alone, but also by electrostatic repulsion between the ZIC-HILIC stationary phase and the glycans. This contributed to the earlier elution of negatively charged glycans. The observed behaviour of negatively charged glycans under the applied conditions was expected due to the low ionic strength of the mobile phase, where the repulsion interaction was not shielded effectively by the eluent counter-ions. The electrostatic repulsion interaction has been previously observed for 2-aminopyridine labelled sialic acid glycans [23]. Under the conditions applied, the proposed hybrid glycans were eluted later than complex biantennary glycans with similar molecular weight, which is in agreement with the previous observation that the high mannose glycans were retained more strongly compared to complex glycans of the same size.

Other minor species observed in the sample were the highly galactosylated complex glycans (l, m), which were eluted after the G2 peak (Table 2). The presence of these glycans in the MAb was consistent with the other species observed in the sample and as expected, their retention times increased with the higher degree of galactosylation. Due to the α-galactosyltransferase activity observed in murine systems, hypergalactosylated glycans with additional α-linked galactose attached to the terminal β-linked galactose can be expected to be found in MAbs expressed in NS0 cell line [39].

The MAb glycans were also analysed under the same separation conditions in negative ionisation mode. For all the neutral and charged glycans, the doubly deprotonated ions were observed (Fig. 5) with the main peaks corresponding to the glycans observed in positive mode. However, the overall sensitivity in negative mode

was lower. In negative mode, better ionisation efficiency for glycans containing sialic acids was expected compared to that of the neutral glycans. The relative peak intensity for the early eluted glycans was higher in negative mode, which additionally confirmed the presence of sialic acids (Fig. 6). The observed ionisation pattern allows the proposed glycan composition to be confirmed with high confidence. The mass spectrum of charged glycans obtained in negative ionisation mode with higher relative intensities for the proposed complex glycans compared to hybrid species (Fig. 6A) was in agreement with the mass spectrum obtained in positive mode (Fig. 4A). Similar relative intensities in positive and negative ionisation mode were observed also for neutral glycans (Figs. 4B and 6B).

The complexity of the sample and the presence of a wide range of minor species required downscaling to enable detailed characterisation of the glycan profile, which is not possible with conventional-scale columns due to the lower sensitivity obtainable. Significant information can therefore be lost when conventional-scale columns are used. Alternatively, separation of fluorescent labelled glycans coupled with fluorescence detection might be necessary in order to ensure adequate sensitivity. Despite some advantages of fluorescence detection, such as high sensitivity and the possibility of relative quantification, this approach does not provide direct information about the structure of glycans and the profiling can be especially challenging when less common glycans are present in the sample. For the analysis of less abundant species the use of high resolution mass spectrometry may be required to confirm the composition with high confidence.

4. Conclusions

We describe here a rapid and sensitive technique for the HILIC separation of reduced high mannose and complex glycans using a nano ZIC-HILIC column coupled with high resolution ESI-TOF-MS. We demonstrate that downscaling can be an efficient way to enhance sensitivity. The new approach allowed glycan profiling without the need for fluorescent labelling. The column exhibited good selectivity for neutral and sialylated glycans and due to the improved sensitivity and high mass accuracy, the composition of several less abundant species could be identified. High resolution mass spectrometry has proven to be a powerful tool in glycosylation analysis as it enables structures with similar composition to be resolved.

Acknowledgements

Support from the Australian Research Council is gratefully acknowledged: PRH the recipient of an ARC Federation Fellowship (FF0668673) and EFH is the recipient of an ARC Future Fellowship (FT0990521).

References

[1] W. Morelle, K. Canis, F. Chirat, V. Faid, J.C. Michalski, Proteomics 6 (2006) 3993.
[2] J.N. Arnold, M.R. Wormald, R.B. Sim, P.M. Rudd, R.A. Dwek, Annu. Rev. Immunol. 25 (2007) 21.
[3] D.H. Dube, C.R. Bertozzi, Nat. Rev. Drug Discov. 4 (2005) 477.
[4] Y. Tian, H. Zhang, Proteom. Clin. Appl. 4 (2010) 124.
[5] M. Butler, Appl. Microbiol. Biotechnol. 68 (2005) 283.
[6] R. Jefferis, Nat. Rev. Drug Discov. 8 (2009) 226.
[7] K. Bork, R. Horstkorte, W. Weidemann, J. Pharm. Sci. 98 (2009) 3499.
[8] L.R. Ruhaak, G. Zauner, C. Huhn, C. Bruggink, A.M. Deelder, M. Wuhrer, Anal. Bioanal. Chem. 397 (2010) 3457–3481.
[9] K.R. Anumula, Anal. Biochem. 350 (2006) 1.
[10] Y. Takegawa, K. Deguchi, T. Keira, H. Ito, H. Nakagawa, S. Nishimura, J. Chromatogr. A 1113 (2006) 177.
[11] G.R. Guile, P.M. Rudd, D.R. Wing, S.B. Prime, R.A. Dwek, Anal. Biochem. 240 (1996) 210.
[12] L.R. Ruhaak, C. Huhn, W.J. Waterreus, A.R. de Boer, C. Neususs, C.H. Hokke, A.M. Deelder, M. Wuhrer, Anal. Chem. 80 (2008) 6119.
[13] J. Qian, T. Liu, L. Yang, A. Daus, R. Crowley, Q.W. Zhou, Anal. Biochem. 364 (2007) 8.
[14] B.D. Prater, H.M. Connelly, Q. Qin, S.L. Cockrill, Anal. Biochem. 385 (2009) 69.
[15] M.P. Campbell, L. Royle, C.M. Radcliffe, R.A. Dwek, P.M. Rudd, Bioinformatics 24 (2008) 1214.
[16] S. Kamoda, R. Ishikawa, K. Kakehi, J. Chromatogr. A 1133 (2006) 332.
[17] J. Stadlmann, M. Pabst, D. Kolarich, R. Kunert, F. Altmann, Proteomics 8 (2008) 2858.
[18] N. Hashii, N. Kawasaki, S. Itoh, M. Hyuga, T. Kawanishi, T. Hayakawa, Proteomics 5 (2005) 4665.
[19] N. Kawasaki, Y. Haishima, M. Ohta, S. Itoh, M. Hyuga, S. Hyuga, T. Hayakawa, Glycobiology 11 (2001) 1043.
[20] L. Mauko, A. Nordborg, J.P. Hutchinson, N.A. Lacher, E.F. Hilder, P.R. Haddad, Anal. Biochem. 408 (2011) 235.
[21] S. Mysling, G. Palmisano, P. Hojrup, M. Thaysen-Andersen, Anal. Chem. 82 (2010) 5598.
[22] J. Wohlgemuth, M. Karas, W. Jiang, R. Hendriks, S. Andrecht, J. Sep. Sci. 33 (2010) 880.
[23] Y. Takegawa, K. Deguchi, H. Ito, T. Keira, H. Nakagawa, S.I. Nishimura, J. Sep. Sci. 29 (2006) 2533.
[24] S. Kamoda, K. Kakehi, Electrophoresis 29 (2008) 3595.
[25] L.A. Gennaro, O. Salas-Solano, Anal. Chem. 80 (2008) 3838.
[26] E. Balaguer, U. Demelbauer, M. Pelzing, V. Sanz-Nebot, J. Barbosa, C. Neusüß, Electrophoresis 27 (2006) 2638.
[27] A. Taichrib, M. Pelzing, C. Pellegrino, M. Rossi, C. Neusüß, J. Proteomics 74 (2011) 958.
[28] M. Wuhrer, C.A.M. Koeleman, A.M. Deelder, C.N. Hokke, Anal. Chem. 76 (2004) 833.
[29] B. Barroso, R. Dijkstra, M. Geerts, F. Lagerwerf, P. van Veelen, A. de Ru, Rapid Commun. Mass Spectrom. 16 (2002) 1320.
[30] N.G. Karlsson, N.L. Wilson, H.-J. Wirth, P. Dawes, H. Joshi, N.H. Packer, Rapid Commun. Mass Spectrom. 18 (2004) 2282.
[31] K.A. Thomsson, M. Bäckström, J.M. Holmén Larsson, G.C. Hansson, H. Karlsson, Anal. Chem. 82 (2010) 1470.
[32] M.S. Bereman, T.I. Williams, D.C. Muddiman, Anal. Chem. 81 (2009) 1130.
[33] M. Ninonuevo, H.J. An, H.F. Yin, K. Killeen, R. Grimm, R. Ward, B. German, C. Lebrilla, Electrophoresis 26 (2005) 3641.
[34] W.R. Alley, M. Madera, Y. Mechref, M.V. Novotny, Anal. Chem. 82 (2010) 5095.
[35] Q. Luo, T. Rejtar, S.-L. Wu, B.L. Karger, J. Chromatogr. A 1216 (2009) 1223.
[36] J.M. Prien, D.J. Ashline, A.J. Lapadula, H. Zhang, V.N. Reinhold, J. Am. Soc. Mass Spectrom. 20 (2009) 539.
[37] I. Nischang, F. Svec, J.M.J. Freĭchet, Anal. Chem. 81 (2009) 7390.
[38] K.N. Baker, M.H. Rendall, A.E. Hills, M. Hoare, R.B. Freedman, D.C. James, Biotechnol. Bioeng. 73 (2001) 188.
[39] D.M. Sheeley, B.M. Merrill, L.C.E. Taylor, Anal. Biochem. 247 (1997) 102.